10.1071/CH19221_AC

Australian Journal of Chemistry 2019, 72(10), 835-841

Supplementary Material

Halogen Functionalization of Aluminium Fumarate Metal-Organic Framework via in-situ Hydrochlorination of Acetylenedicarboxylic Acid

Tobie J. Matemb Ma Ntep,[A] Wei Wu,[A] Hergen Breitzke,[B] Carsten Schlüsener,[A] Bastian Moll,[A] Laura Schmolke,[A] Gerd. Buntkowsky [B] and Christoph Janiak[A,C]

[A] Institut für Anorganische Chemie und Strukturchemie, Heinrich-Heine-Universität Düsseldorf, Universitätsstraße 1, D- 40225 Düsseldorf, Germany

[B] Eduard-Zintl-Institut für Anorganische und Physikalische Chemie, Technische Universität Darmstadt, Alarich-Weiss-Straße. 4, D-64287 Darmstadt, Germany

[C] Corresponding author: E-mail: janiak@uni-duesseldorf.de; Fax: + 49-211-81-12287; Tel: +49-211-81-12286

Additional email addresses:
tobie.matemb.ma.ntep@uni-duesseldorf.de; wei.wu@uni-duesseldorf.de; breitzke@chemie.tu-darmstadt.de; laura.schmolke@uni-duesseldorf.de; carsten.schluesener@uni-duesseldorf.de; bastian.moll@uni-duesseldorf.de; gerd.buntkowsky@chemie.tu-darmstadt.de

Table of contents

Materials, syntheses and methods

Acetylenedicarboxylic acid Acetylenedicarboxylic acid (H_2ADC, purity 97%) was purchased from Alfa Aesar; aluminium chloride hexahydrate ($AlCl_3$, purity 99%) was purchased from Janssen Chimica; N,N-dimethylformamide (DMF, analytical reagent grade) and Ethanol (analytical reagent grade) were purchased from Fischer Chemical; acetic acid (purity >99%) was purchased from VWR Chemicals. All reagents were used as purchased, without further purification.

Synthesis procedure of aluminium chlorofumarate (MIL-53-Fum-Cl)

Al-MIL-53-Fum-Cl was synthesized by mixing $AlCl_3 \cdot 6H_2O$ (483 mg, 2 mmol), H_2ADC (228 mg, 2 mmol), 50 mL DMF and 5 mL acetic acid as modulator in a 100 mL Duran bottle with a screw cap, which was heated at 85 °C for 72 h. light brown/yellowish powder was isolated from brown mother liquor by centrifugation and washed three times with fresh 5mL DMF, followed by washing three times with 5mL ethanol. After centrifugation, the product was allowed to dry at room temperature in air. The as-synthesized material was heated 7h at 150 °C under dynamic vacuum to yield the activated material. Yield = 296 mg (77%) based on the aluminium salt.

Synthesis procedure of aluminium fumarate (MIL-53-Fum)

Aluminium fumarate was synthesized according to a previously reported method.[1] In short, 513 mg of $Al_2(SO_4)_3 \cdot 18H_2O$, 179 mg fumaric acid and 92 mg urea were dissolved in 5 mL water, sealed in a Teflon lined autoclave and heated for 32 h at 110 °C in an oven. The resulting powder was washed with water and ethanol. It was activated by heating 7 h at 150 °C under dynamic vacuum.

Methods

All **powder X-ray (PXRD)** patterns were acquired using a Bruker D2 Phaser diffractometer equipped with a flat sample holder (also a flat silicon, low background sample holder). The devise operates with Cu $K\alpha_1/\alpha_2$ radiation λ = 1.5418 Å at 30 kV covering 2theta angles 5-50° over a time of 1 h, that is 0.0125 °/sec.

Raman spectroscopy was executed on a Bruker MultiRAM-FT Raman spectrometer equipped with a Nd:YAG-laser (wavelength 1064 nm). All Raman spectra were measured in solid state for 2500 scans with a laser power between 10-20 mW.

Infrared spectroscopy was done using a Bruker FT-IR Tensor 37 Spectrometer in the 4000-550 cm^{-1} region with 2 cm^{-1} resolution as KBr disks.

Thermogravimetric analysis (**TGA)** was performed using a Netzsch TG 209 F3 Tarsus thermal analyser under an air flow with a heating rate of 5 °C min^{-1}.

Conventional **CP MAS solid state NMR** measurements were carried out at room temperature on a Bruker AVANCE II+ spectrometer at 400 MHz proton resonance frequency, employing a Bruker 4 mm double resonance probe. ^{13}C CP MAS spectra were recorded utilizing ramped CP-MAS sequences at spinning rates of 8 kHz. Contact time was set to 1.5 ms and tppm decoupling with a 15° phase jump was applied during data acquisition.[2] ^{13}C spectra were referenced with respect to

TMS (tetramethylsilane). Frequency switched Lee Goldburg (FSLG) CP MAS HETCOR spectra were recorded at 8 kHz and contact times of 2 ms, 500 µs and 200 µs. The tppm decoupling sequence with a 15° phase jump was applied during data acquisition. ^{1}H spectra were recorded utilizing FSLG homonuclear decoupling, applying the same LG field strength and step width as for the FSLG HETCOR spectra. ^{1}H shift values of the direct dimension of these spectra were utilized to reference the indirect dimensions of the FSLG HETCOR spectra. The direct dimensions of the ^{1}H spectra were referenced with respect to TMS.

Liquid ^{1}H, ^{13}C NMR spectra were measured with a Bruker Avance III-300 (300 MHz). Prior to solution NMR analysis, an activated sample of MIL-53-Fum-Cl was digested as follows: 20 mg of MOF were suspended in water free DMSO-d_6 (0.65 mL). 5 drops of DCl (35 wt% in D_2O) were added. After 3 h, the yellowish supernatant solution was separated from the decanted white solid of aluminium oxide and introduced in the NMR tube for analysis.

X-ray photoelectron spectroscopy (XPS) was performed with an ULVAC-PHI VersaProbe II microfocus X-ray photoelectron spectrometer. The spectra were recorded using polychromatic aluminum Kα X-ray source (1486.8 eV) and referenced to the carbon 1s orbital with a binding energy of 284.8 eV. Fitting of the experimental XP spectra was done with the program CasaXPS, version 2.3.19PR1.0, copyright 1999-2018 Casa Software Ltd.

Scanning electron microscopy (SEM) images were obtained using a Jeol JSM-6510LV QSEM advanced electron microscope with a LaB_6 cathode at 5–20 keV. The samples for SEM imaging were coated with gold using a Jeol JFC 1200 fine-coater (20 mA for 25 s).

For **gas sorption studies** N_2, H_2, CH_4 and CO_2 isotherms were measured on a Quantachrome Autosorb iQ MP at 77 K (N_2, H_2) and 273 K (CH_4, CO_2), respectively. The specific surface area was calculated from the nitrogen sorption isotherms using the Brunauer-Emmett-Teller (BET) equation. All gases for the sorption measurements were of ultrapure grades (99.999%, 5.0).

Water vapor sorption isotherms were measured gravimetrically at 20 °C on a VSTAR^{TM} vapor sorption analyzer (Model number Vstar4-0000-1000-XS) from Quantachrome. For this purpose, about 25 mg of activated sample were introduced in the measuring cell and connected to the analysis port of the analyzer.

Infrared and Raman spectra of MIL-53-Fum-Cl and MIL-53-Fum

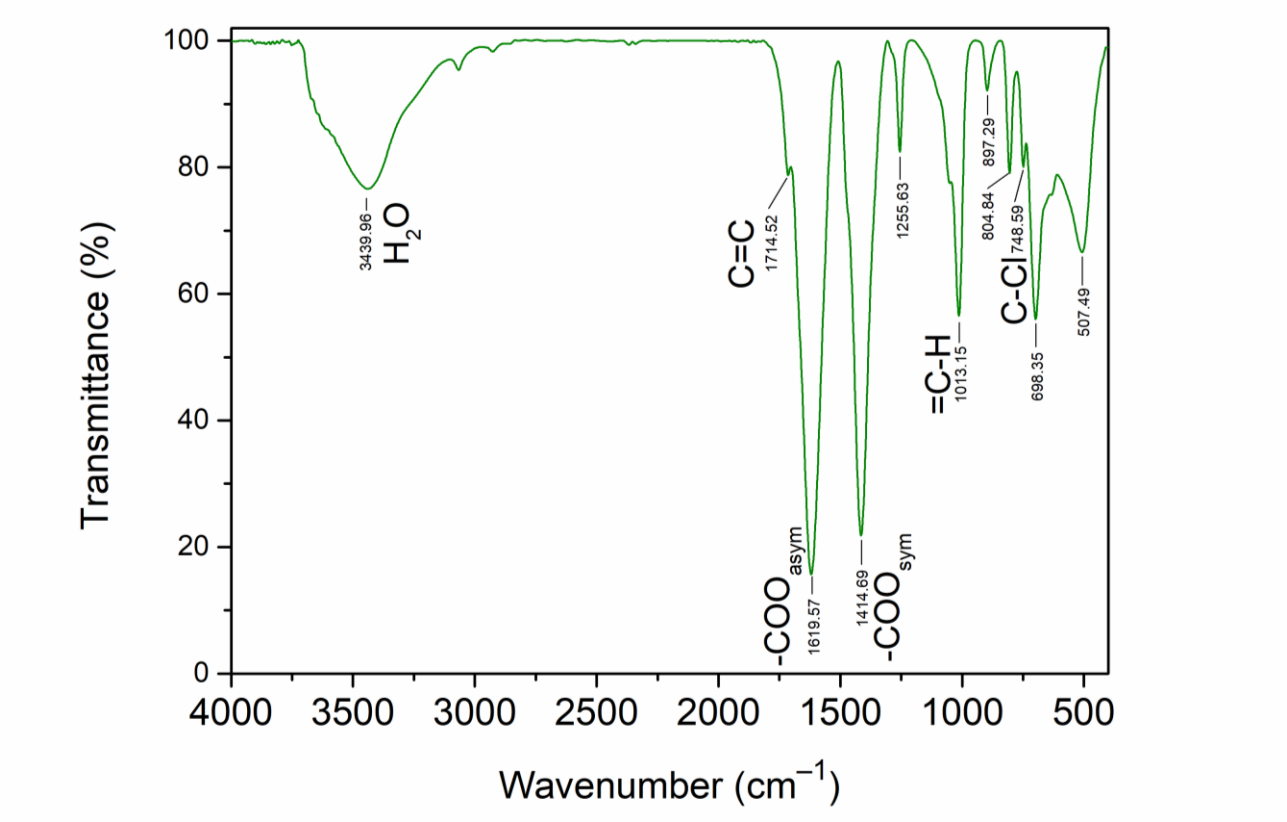

Fig. S1 Infrared spectrum of MIL-53-Fum-Cl.

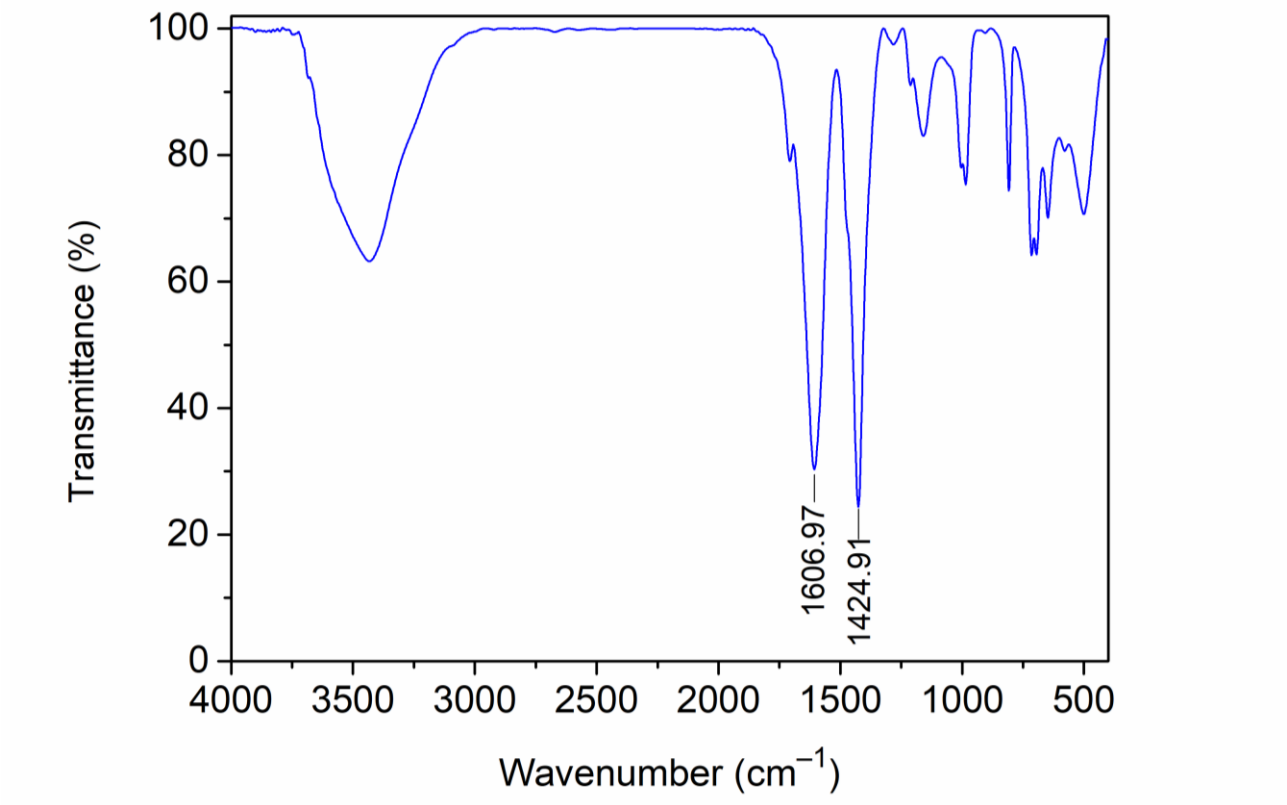

Fig. S2 Infrared spectrum of aluminium fumarate (MIL-53-Fum).

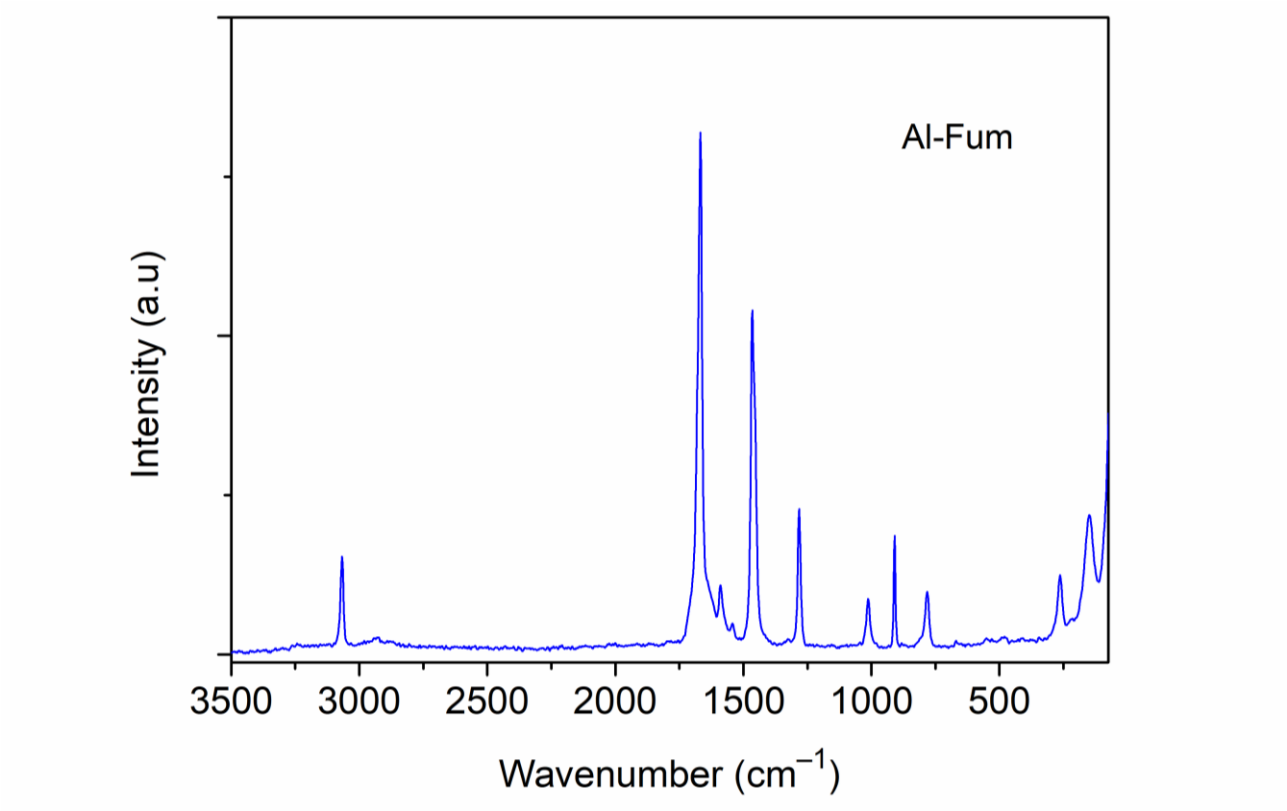

Fig. S3 Raman spectrum of aluminium fumarate.

Solid-state ^{1}H spectrum of MIL-53-Fum-Cl

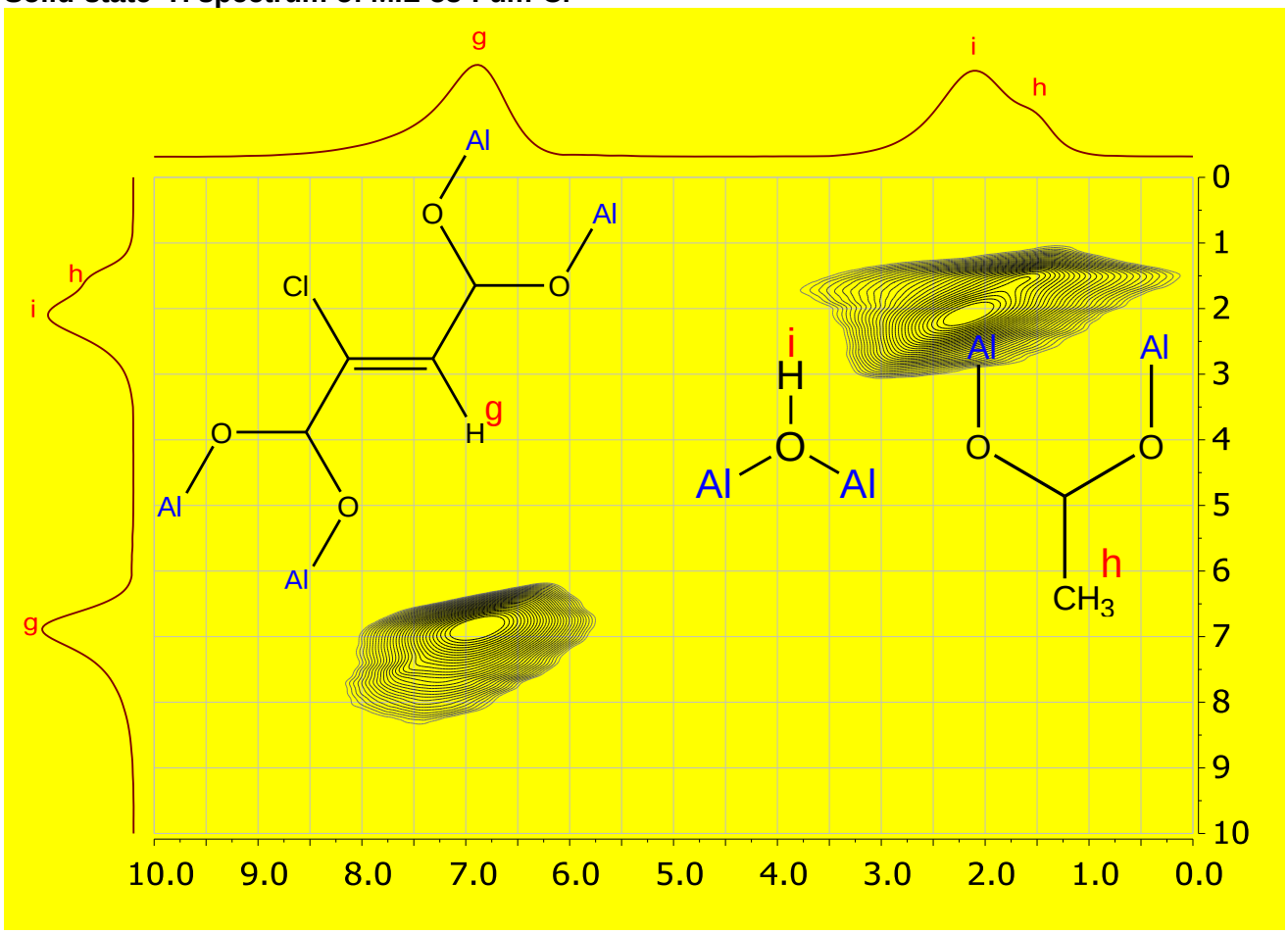

Fig. S4 Homonuclear decoupled 2D FSLG proton (^{1}H-^{1}H) spectrum at 8 kHz spinning speed and 200 µs contact time of MIL-53-Fum-Cl.

Liquid ^{1}H and ^{13}C NMR spectra of MIL-53-Fum-Cl

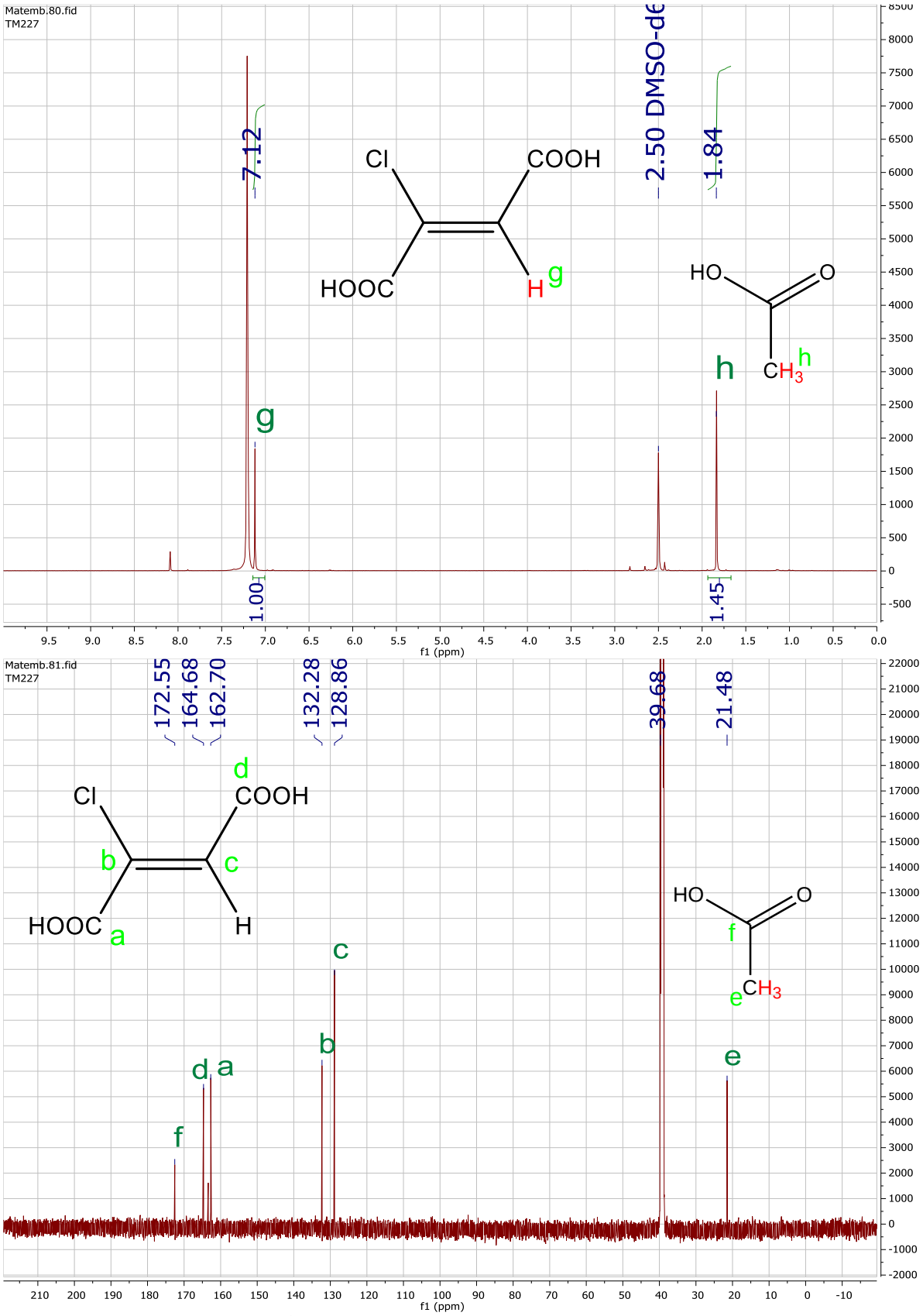

Fig. S5 Liquid ^{1}H (top) and ^{13}C (bottom) NMR spectra of digested Al-Fum-Cl in DMSO-d_6.

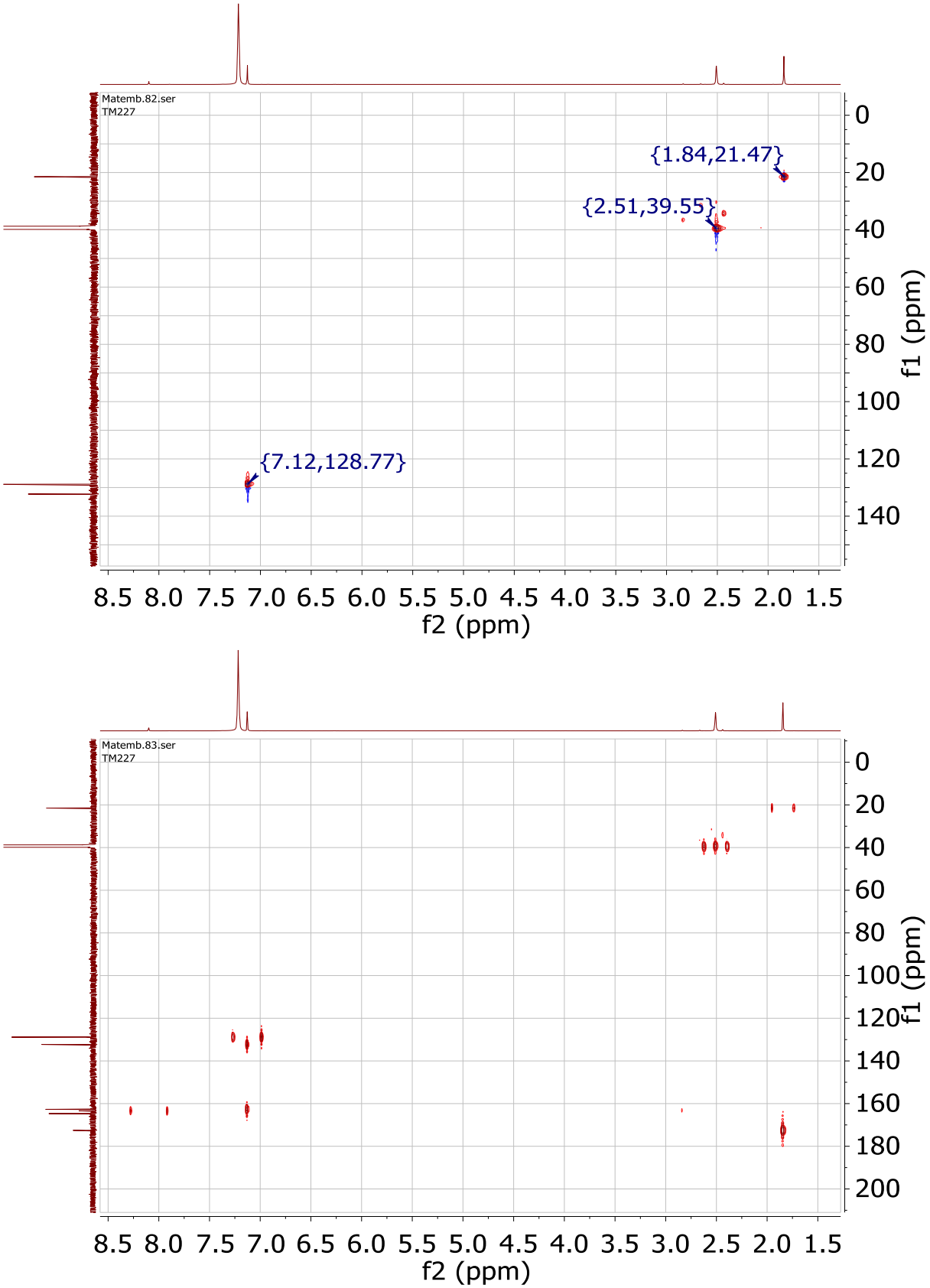

Fig. S6 2D ^{1}H-^{13}C HSQC (top) and HMBC (bottom) NMR spectra of digested MIL-53-Fum-Cl in water free DMSO-d_6. HSQC = Heteronuclear Multiple Quantum Correlation, HMBC = Heteronuclear Multiple Bond Correlation.
HSQC correlates the chemical shift of protons with chemical shift of the directly bonded carbons. HMBC gives correlations between protons and carbons that are separated by two or three bonds (direct one-bond correlations are suppressed).

Determination of missing linker ratio in MIL-53-Fum-Cl MOF from liquid ^{1}H NMR

$$\frac{Acetate}{Fum-Cl}\text{molar ratio} = \frac{\left(\frac{Integration\ of\ acetate\ signal}{Number\ of\ protons\ per\ acetate}\right)}{\left(\frac{Integration\ of\ Fum-Cl\ signal}{Number\ of\ protons\ per\ Fum-Cl}\right)}$$
$$= \left(\frac{Integ.of\ acet.}{3}\right) \times \left(\frac{1}{Integ.of\ Fum-Cl}\right)$$

Hence, the acetate to linker molar ratio is calculated to 0.689.

Considering the unit formula $[Al(OH)_{1+x}(Fum\text{-}Cl)_{1-x}(Ac)_x]$ where *x* is the number of missing linker per unit formula:

$$\frac{Ac}{Fum-\mathrm{x}}\text{molar ratio} = m_R = \frac{x}{1-x}\ , \qquad \text{which leads to} \quad x = \frac{m_R}{1+m_R}$$

The corresponding amount of missing linker per unit formula is 0.4.

Energy dispersive X-ray spectroscopy (EDX) of MIL-53-Fum-Cl

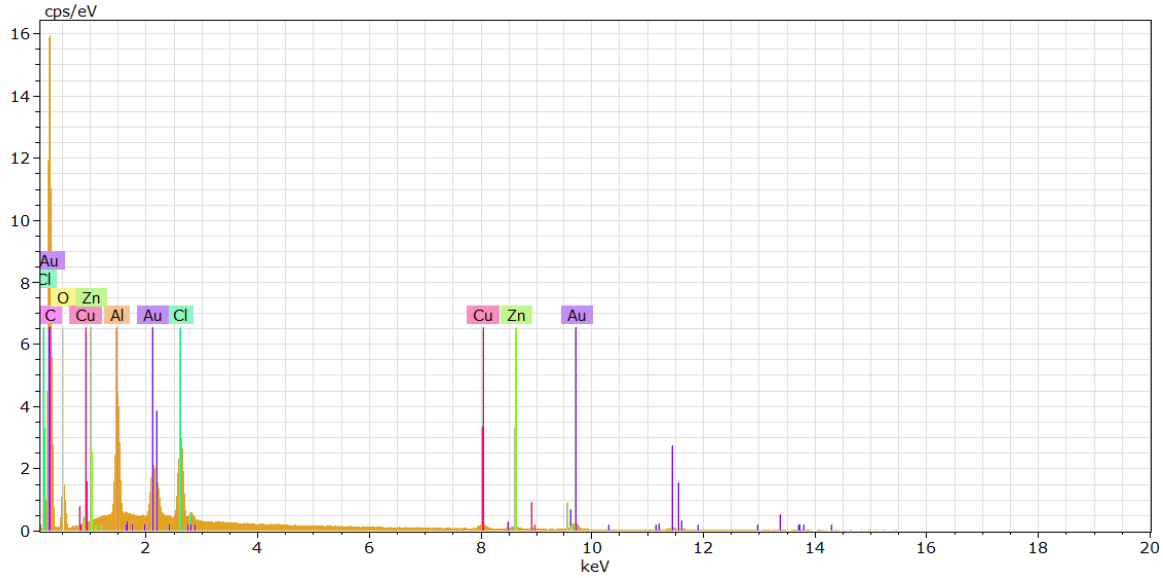

Fig. S7 EDX spectrum of MIL-53-Cl.

Table S1. Atom and Weight % of C, O, Cl and Al for MIL-53-Fum-Cl

Element [a]	atom#	Series	mass fraction [wt.%]	[norm. wt.%]	atom fraction [norm. At.%]	standard deviation for wt.% (1 Sigma)
C	6	K-Series	62.5	70.6	85.6	7.3
O	8	K-Series	9.8	11.1	10.1	1.5
Al	13	L-Series	2.8	3.12	1.7	0.2
Cl	17	L-Series	2.7	3.04	1.2	0.1
Au	79	L-Series	8.4	9.4	0.7	0.3
Cu	29	K-Series	1.3	1.5	0.3	0.1
Zn	30	K-Series	1	1.1	0.3	0.1
		Summe:	96.04	100	100	

[a] The element signals for Au, Cu, Zn stem from the sputtering and brass sample holder.

X-ray photoelectric spectroscopy (XPS) of MIL-53-Fum-Cl

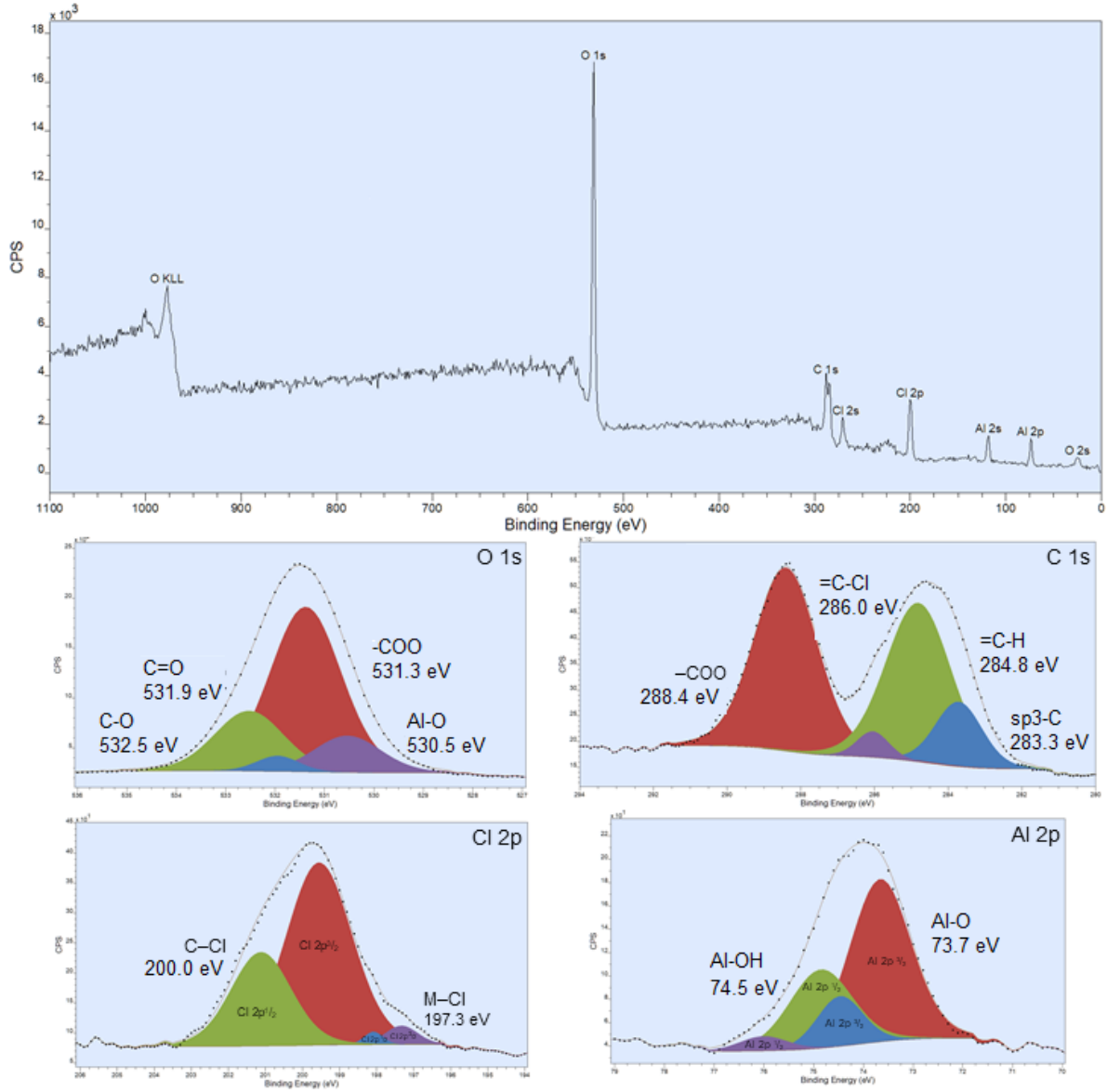

Fig. S8 XPS survey spectrum of MIL-53-Fum-Cl and high resolution core-level in the region of O 1s, C 1s, Cl 2p and Al 2p.

The structure of new material consists therefore of chains Al atoms bridged by two chlorofumarate linkers and one μ-OH (Fig. 3). The obtained material is therefore a chloro-functionalized version of aluminium fumarate, that is, MIL-53-Fum-Cl consists of *trans*-corner sharing AlO_6 octahedra, linked together by chlorofumarate to form lozenge-shaped one-dimensional chloro-decorated pores.

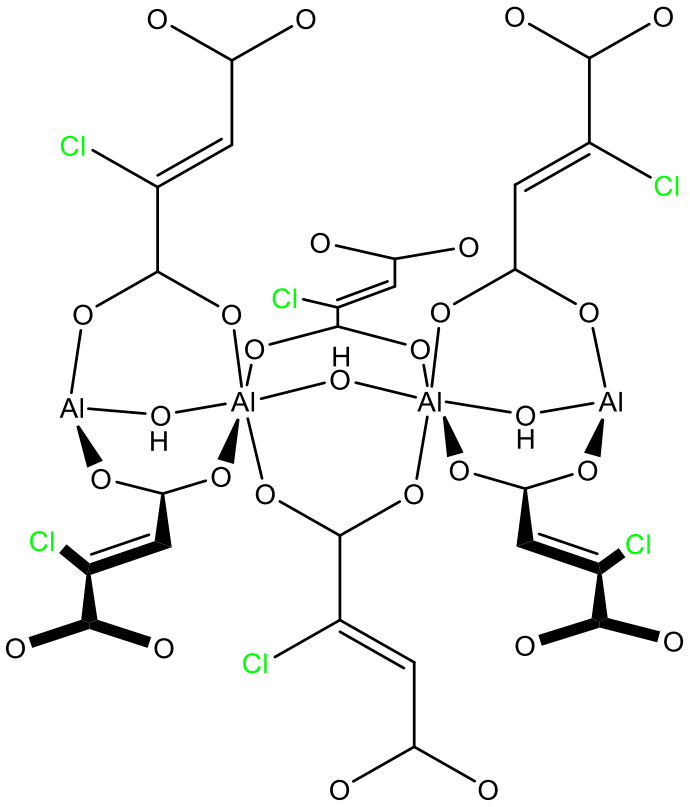

Fig. S9 Structural building block of MIL-53-Fum-Cl framework.

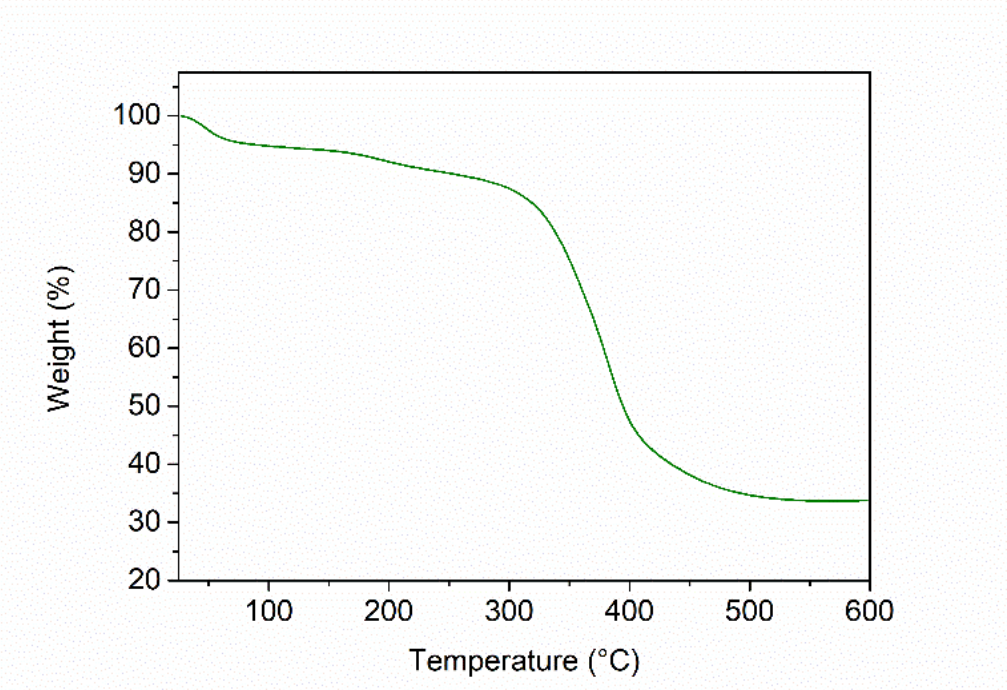

Fig. S10 Trace of thermogravimetric analysis under air for MIL-53-Fum-Cl.

Missing linker defect calculation

The ideal (defect-free) **MIL-53-Fum-Cl** (Al-Fum-Cl) MOF formula would be [Al(OH)(Fum-Cl)]

The desolvated form Al(OH)(Fum-Cl) would yield 0.5 equivalents Al_2O_3 as a solid residue upon complete decomposition under air.

The equivalent mass of the solid residue would be: 0.5 × M(Al_2O_3) = 50.98 g

The molar mass of ideal **MIL-3-Fum-Cl**: M[Al(OH)(Fum-Cl)] = 192.49 g mol^{-1}, is a factor of 3.78 higher than the solid residue.

The ideal plateau of the desolvated MOF should then be found at 378% on the TG trace normalized to 100% solid residue i.e $Wt_{ideal\ plat.}$ = 378% and W_{end} = 100% (Fig. S11).

The experimental plateau of the final desolvated MIL-53-Fum-Cl is found at a weight loss of $Wt_{exp.plat.}$ = 268% (Fig. S11).

A value for expected weight loss is:

$Wt_{pL.theo}$ = ($Wt_{ideal\ plat.}$ – W_{end}) = (378 – 100) / 6 = 278%

The number of experimental linkers (x = number of linker deficiency) per formula unit is:

$NL_{exp.}$ = 1 – x = ($Wt_{exp.\ plat.}$ - W_{end}) / $Wt_{pL.theo}$ = (268 – 100) / 278 = 0.6 and then the number of linker deficiency per formula unit is x = 0.4 which is the same value found from NMR analysis.

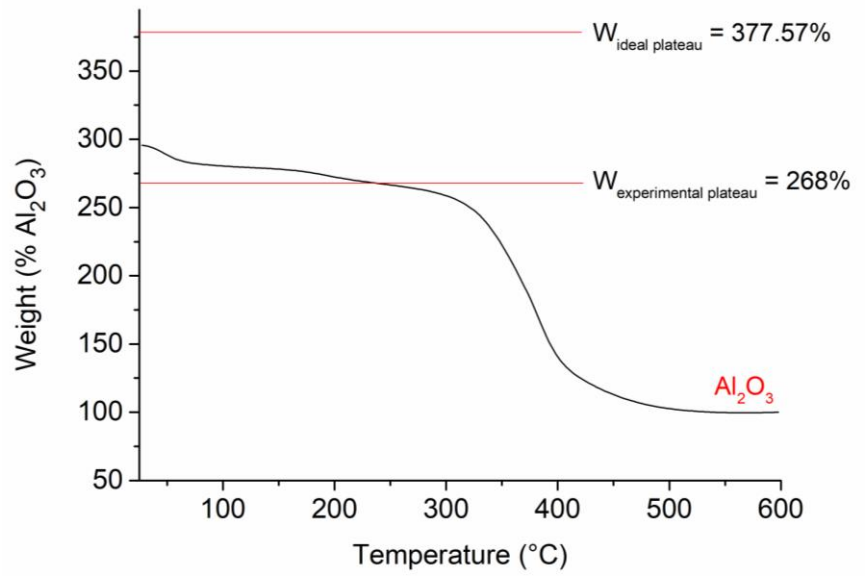

Fig. S11 Normalized TGA curve of MIL-53-Fum-Cl.

PXRD patterns of the chemical stability testing

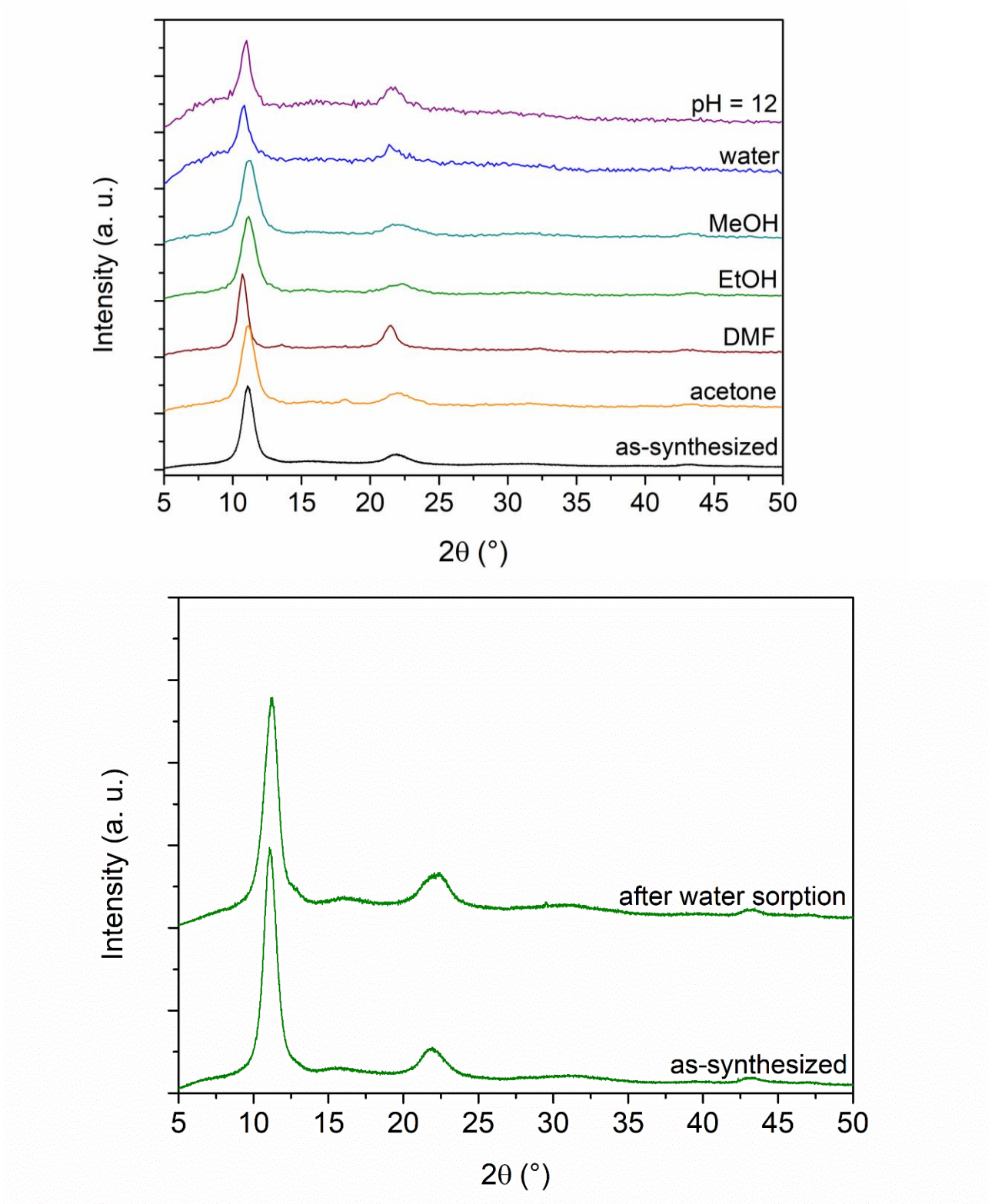

Fig. S12 PXRD patterns of MIL-53-Fum-Cl after stirring 24 h at room temperature in various solvents and solutions (top). PXRD of MIL-53-Fum-Cl after water sorption experiment (bottom).

Nitrogen sorption isotherms and porosities of MIL-53-Fum-Cl and MIL-53-Fum

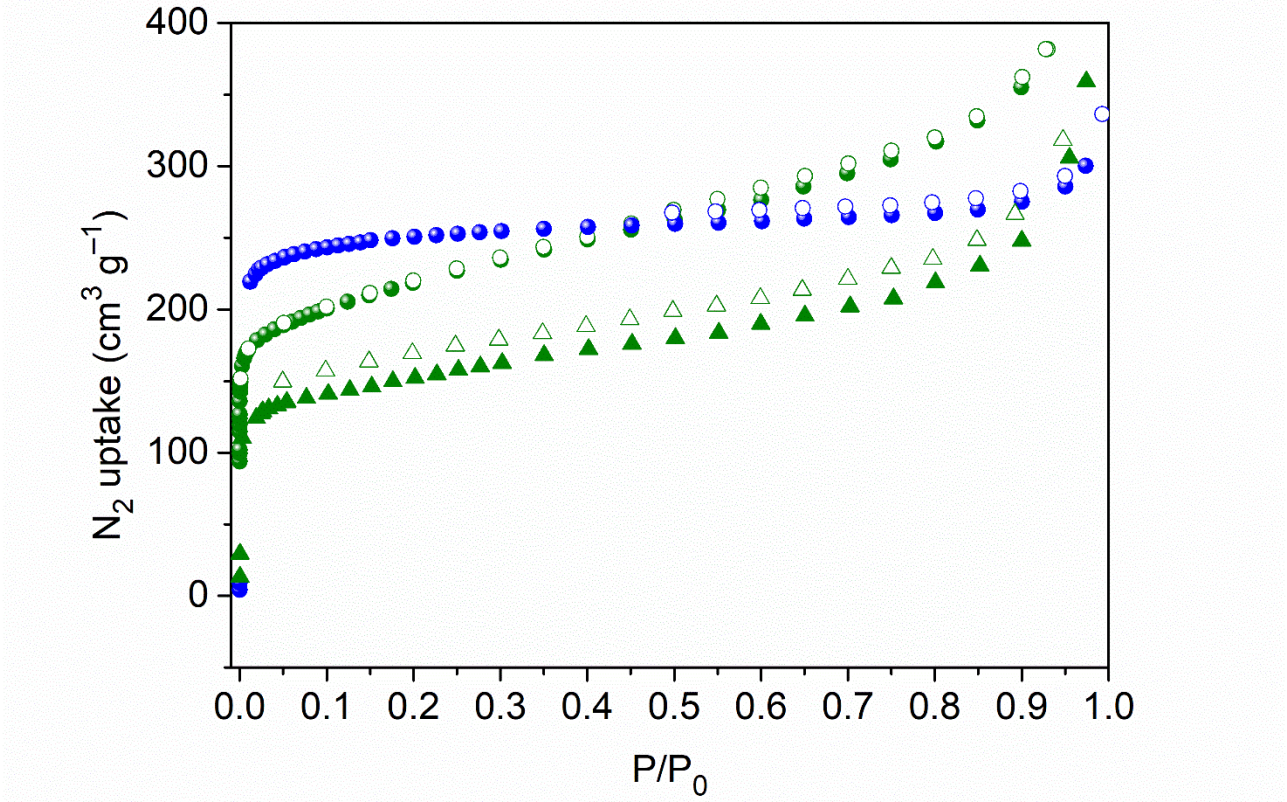

Fig. S13 Nitrogen sorption isotherms of MIL-53-Fum-Cl (green; circles before water sorption; triangle after water sorption) and MIL-53-Fum (blue) (filled symbols: adsorption; empty symbols: desorption).

For MIL-53-Fum-Cl the N_2 isotherm in Fig. S12 is of Type Ib at lower and Type II at higher relative pressure, the latter due to interparticle macropore condensation. The isotherm of aluminium fumarate (MIL-53-Fum) features a type I typical for microporous materials.

Table S2. Surface area and porosity parameters of MIL-53-Fum-Cl and MIL-53

Adsorptive	S_{BET} (m^2g^{-1}) [a]	$S_{micro\text{-}BET}$ (m^2g^{-1}) [b]	S_{Ext} (m^2g^{-1}) [c]	$V_{pore\ (total)}$ (cm^3g^{-1}) [d]	$V_{pore\ (micro)}$ (cm^3g^{-1}) [e]
MIL-53-Fum-Cl	800	551	249	0.48	0.21
MIL-53-Fum-Cl aft. wat. sorp.	570	315	255	0.38	0.12
MIL-53-Fum	982	864	118	0.42	0.33

[a] BET surface areas (S_{BET}) were obtained from five adsorption points in the pressure range pp_0^{-1}=0.001-0.05. [b] Micropore areas ($S_{micro\text{-}BET}$) were obtained by t-plot and V-t-method. [c] External area (S_{Ext}) refers to all area that does not originate from micropores and it includes meso- and macropores, i.e. pores > 2nm. Obtained by t-plot and V-t-method. [d] Total pore volumes ($V_{pore\ (total)}$) were derived at pp_0^{-1} = 0.95 for pores ≤ 20 nm. [e] Micropore volume ($V_{pore\ (micro)}$) refers to volume that originates only from micropores, obtained by V-t-method with thickness method 'DeBoer'. All correlation coefficients (r) within calculations were >0.999.

Fitting of CO_2, CH_4 and H_2 isotherms

Fits of adsorption isotherms were performed using the software **3P**Sim software.[3] **3P**Sim is a tool for interpretation and evaluation of experimental data from equilibrium and dynamic experiments. Several adsorption isotherm models including Henry, Toth, Freundlich, LAI, SIPS, Dual-site Langmuir, and DS Langmuir SIPS models. The isotherm model was validated based on the best correlation coefficient R^2. For the best fitting adsorption model, were calculated the affinity constant, the exponent and maximal loading. The Toth was the best fitting model for CO_2 and CH_4 isotherms, whereas the Sips model was the best to fit H_2 isotherms.

The Toth equation has the form is given by the equation 1

$$q = q_{max} \cdot \frac{k \cdot p}{[1 + (k \cdot p)^t]^{1/t}} \qquad (1)$$

Where q is the amount adsorbed, q_{max} is the amount adsorbed at saturation / maximal loading, p is the equilibrium pressure, k is the Toth constant and t the Toth exponent. k and t describe the heterogeneity of the adsorbent surface.[4]

The Sips equation is given by the equation 2

$$q = q_{max} \cdot \frac{(k \cdot p)^t}{1 + (k \cdot p)^t} \qquad (2)$$

q is the gas amount adsorbed (mmol g^{-1}); q_{max} is the maximum loading; k is the affinity constant (bar^{-1}); t is the heterogeneity exponent; p is the pressure (bar).

The obtained fits are shown in Fig. S14 and the different parameter obtained are presented in Table S3 below.

The IAST (ideal adsorbed solution theory) calculation was done with the multicomponent IAST-Toth model. The mole fraction of 0.5 was set for each gas and the parameters (affinity constant, saturation capacity, exponent) obtained from the Toth fit were given as input, as well as the total pressure of 1 bar. The respective adsorbed fractions of CO_2 (x_1) and CH_4 (x_2) were generated from which the selectivity was calculated using the formula:

$$S = \frac{x_1/x_2}{y_1/y_2}$$

y_1 and y_2 are the mole fractions respectively of CO_2 and CH_4 in the adsorptive i.e $y_1 = y_2 = 0.5$ for our 50:50 gas mixture. x_1 = 0.895 and x_2 = 0.105 for MIL-53-Fum-Cl; x_1 = 0.819 and x_2 = 0.181 for MIL-53-Fum.

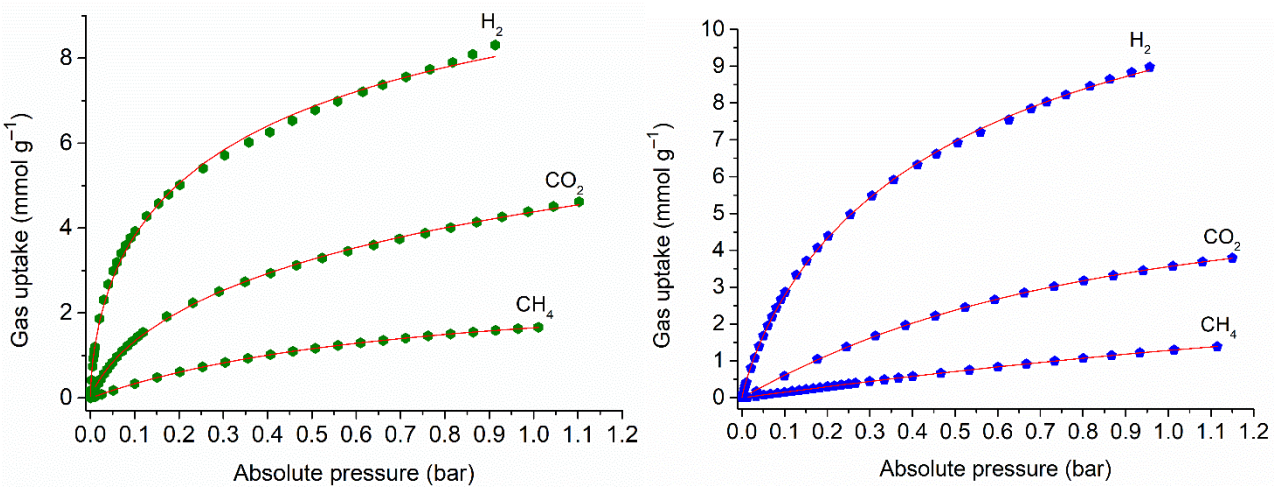

Fig. S14 Experimental CO_2, CH_4 and H_2 adsorption isotherms of MIL-53-Fum-Cl (green, left) and MIL-53-Fum, with corresponding Toth (CO_2 & CH_4, 273 K) or Sips (H_2, 77 K) model fits.

Table S3. Obtained Toth/Sips fitting parameters of CO_2 CH_4 and H_2 adsorption isotherms for MIL-53-Fum-Cl and MIL-53-Fum.

	MIL-53-Fum-Cl			**MIL-Fum**		
Gas	CO_2	CH_4	H_2	CO_2	CH_4	H_2
Toth/sips exponent	0.445	1.060	0.59	1.29	1.43	0.85
correlation coefficient R^2	0.999	0.999	0.998	0.999	0.999	0.999
affinity constant / bar^{-1}	2.73	1.34	2.18	1.09	0.41	1.87
maximal loading / mmol g^{-1} [a]	13.29	2.76	13.34	5.81	3.68	14.314

[a] amount adsorbed at saturation, that is maximal loading for the asymptotic curvature of the adsorption isotherm.

Determination of the isosteric heat of CO_2 adsorption

The CO_2 isotherms experimentally obtained respectively at 273 K and 298 K were fitted with the Langmuir-Freundlich model (eq. 1). The fits are shown in Fig. S15. The obtained fits were used to determine the pressure for each temperature corresponding to various CO_2 loadings. The isosteric heat of adsorption was finally calculated by applying the Clausius-Clapeyron equation (eq. 2).

$$q = q_{max} \cdot \frac{(k \cdot p)^t}{1 + (k \cdot p)^t} \qquad (1)$$

q is the gas amount adsorbed (mmol g^{-1}); q_{max} is the maximum loading; k is the affinity constant (bar^{-1}); t is the heterogeneity exponent; p is the pressure (kPa).

$$Q_{st} = -R\left(\frac{T_2 T_1}{T_2 - T_1}\right) ln \frac{P_2}{P_1} \qquad (2)$$

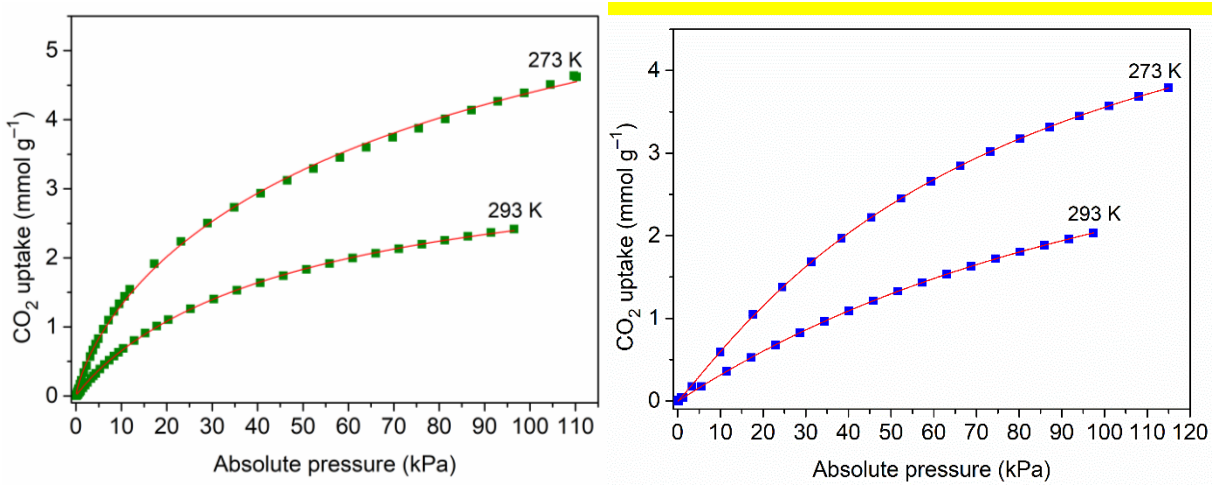

Fig. S15 Fitting of CO_2 adsorption isotherms with the Langmuir-Freundlich model for MIL-53-Fum-Cl (left, green) and MIL-53-Fum (right, blue). Symbols for experimental data and red lines for simulated fits.

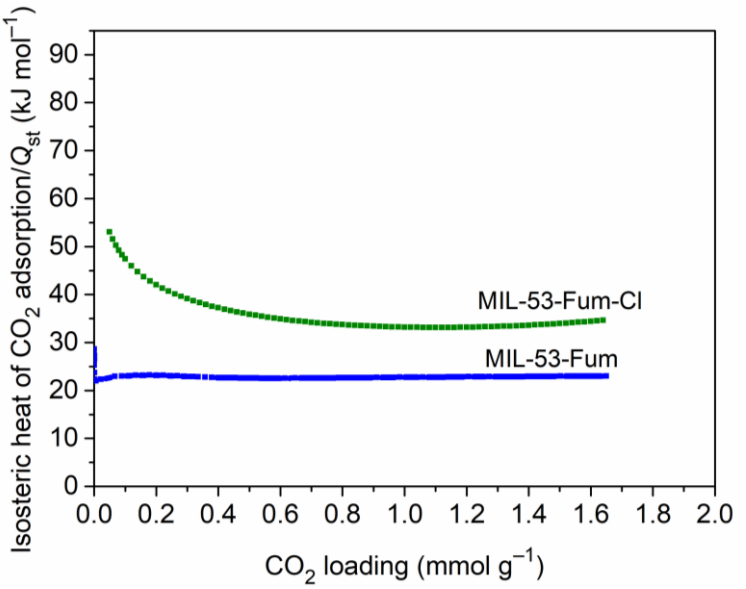

Fig. S16 Plot of isosteric heat of CO_2 adsorption for MIL-53-Fum-Cl (green) and MIL-53-Fum (blue) from isotherms data at 273 and 293 K.

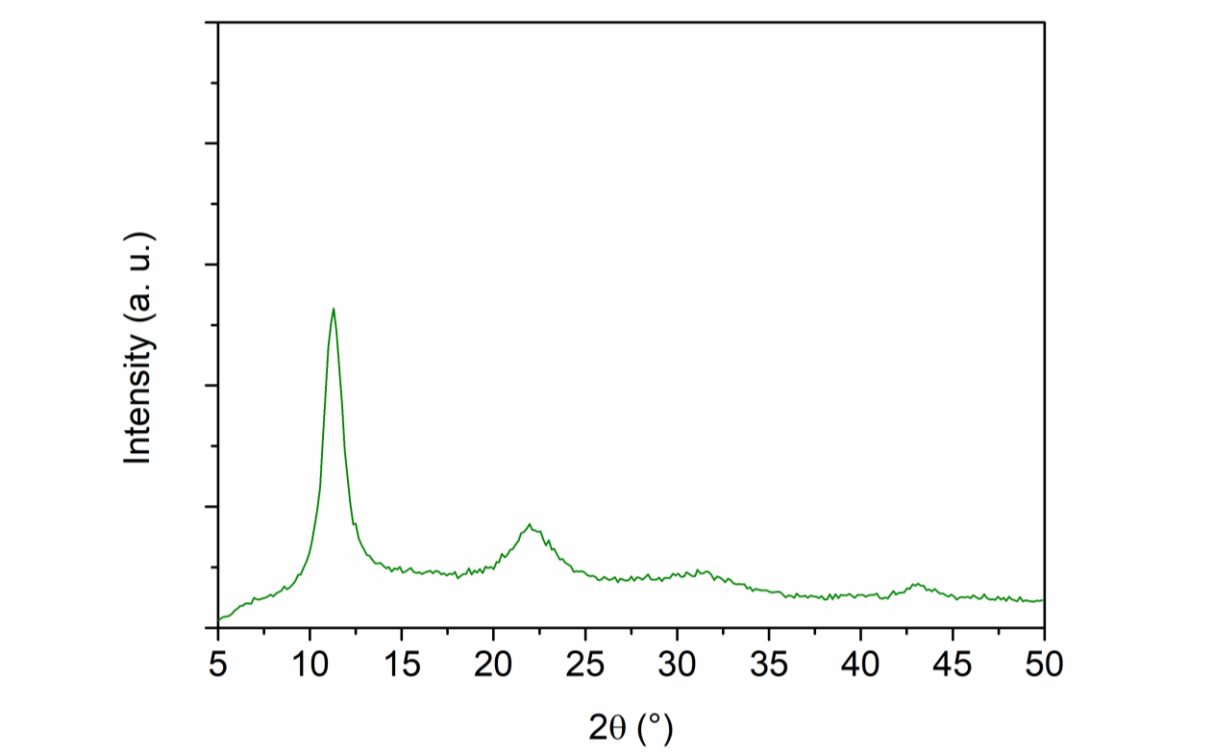

Fig. S17 PXRD pattern of MIL-53-Fum-Cl synthesized with formic acid modulator.

Discussion on the extra reflection at ~13° 2θ in the PXRD pattern of MIL-53-Fum

Examination of experimental PXRDs in the literature for MIL-53-Fum (= aluminium fumarate) and the related Ga-fumarate can exhibit a reflection at ~13° and ~15° 2θ angle. Often but not always the reflection at ~13° disappears and the reflection at ~15° shifts to slightly lower angle upon activation or samples where the original solvent has been exchanged with water (Fig. S18-S19 in Suppl. Mater.). Noteworthy, activation of MIL-53-Fum with increasing temperature (re-)introduces the peak at ~13° when starting from a most likely water-containing sample which only showed one peak at 2θ slightly below 15° (Fig. S20 in Suppl. Mater.).

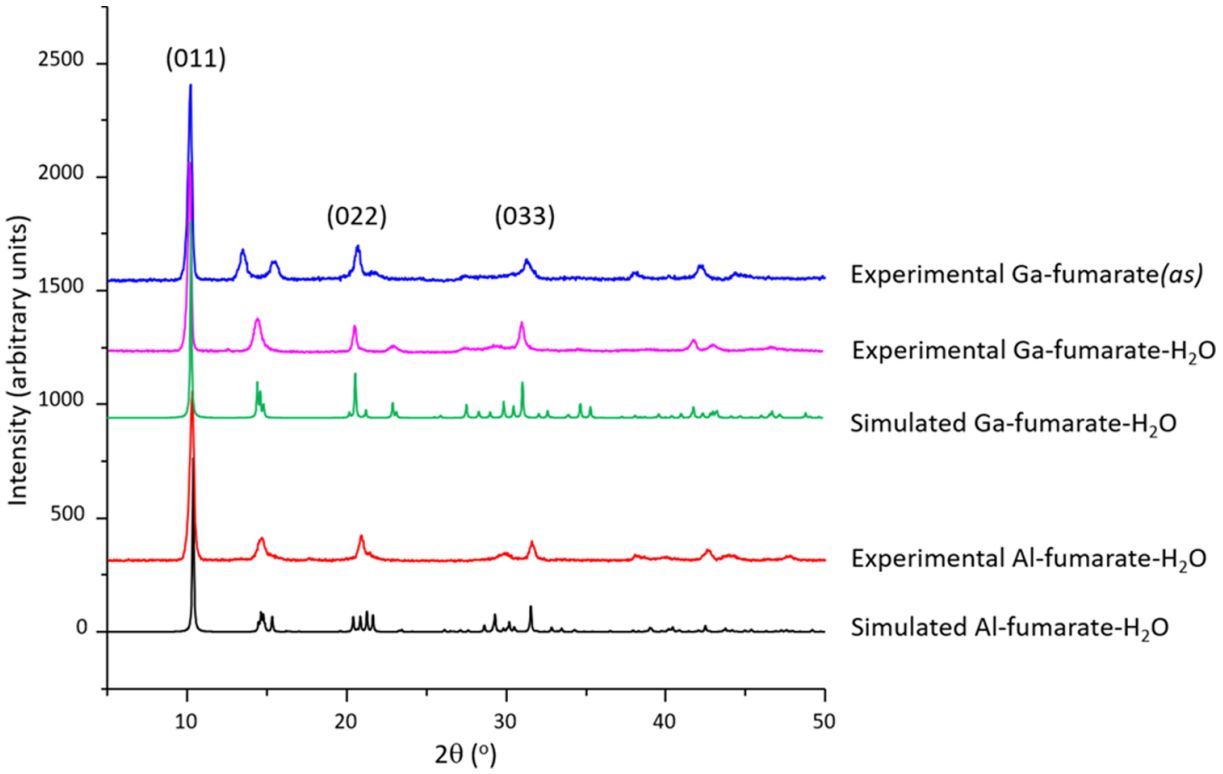

Fig. S18 Comparison of simulated and experimental PXRD patterns of Al- and Ga-fumarate MOFs, with select reflections labeled. The samples with water adsorbed within the channels are termed Al-fumarate−H_2O and Ga-fumarate−H_2O, respectively. The as-made sample of Ga-fumarate is referred to as Ga-fumarate(as). The 0kk reflections of Ga-fumarate−H_2O are shifted to lower angles versus those of Ga-fumarate(as), which indicates a small contraction of the MOF channel that propagates along the direction of the fumarate linker. Note the x-axis is truncated to exclude angles below 5°. Reprinted with permission from ref. Y. Zhang, B. E. G. Lucier S. M. McKenzie, M. Arhangelskis, A. J. Morris, T. Friščić, J. W. Reid, V. V. Terskikh, M. Chen, Y. Huang, *ACS Appl. Mater. Interfaces*, **2018**, *10*, 28582–28596. Copyright 2018 American Chemical Society.

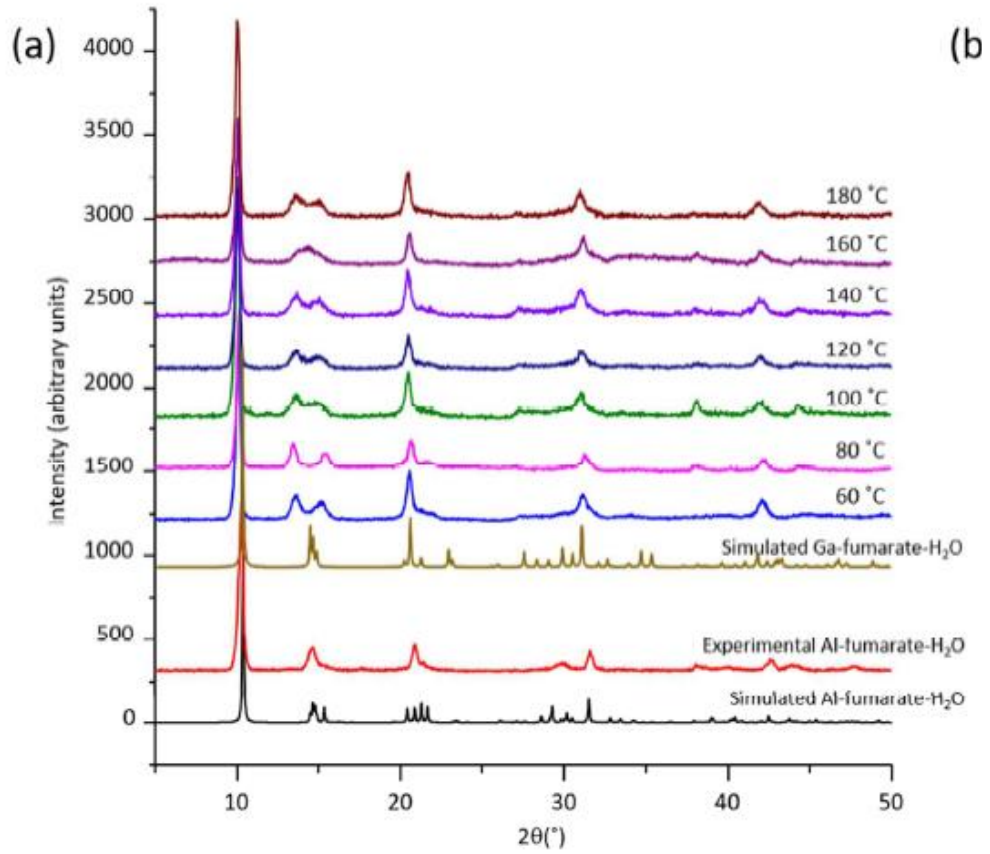

Fig. S19 The experimental PXRD patterns of as-synthesized Ga-fumarate prepared at temperatures ranging from 60 °C to 180 °C, along with experimental and simulated Al-fumarate-H_2O and simulated Ga-fumarate-H_2O PXRD patterns; all simulations were calculated from the corresponding crystal structures. Reprinted with permission from ref. Y. Zhang, B. E. G. Lucier S. M. McKenzie, M. Arhangelskis, A. J. Morris, T. Friščić, J. W. Reid, V. V. Terskikh, M. Chen, Y. Huang, *ACS Appl. Mater. Interfaces*, **2018**, *10*, 28582–28596. Copyright 2018 American Chemical Society.

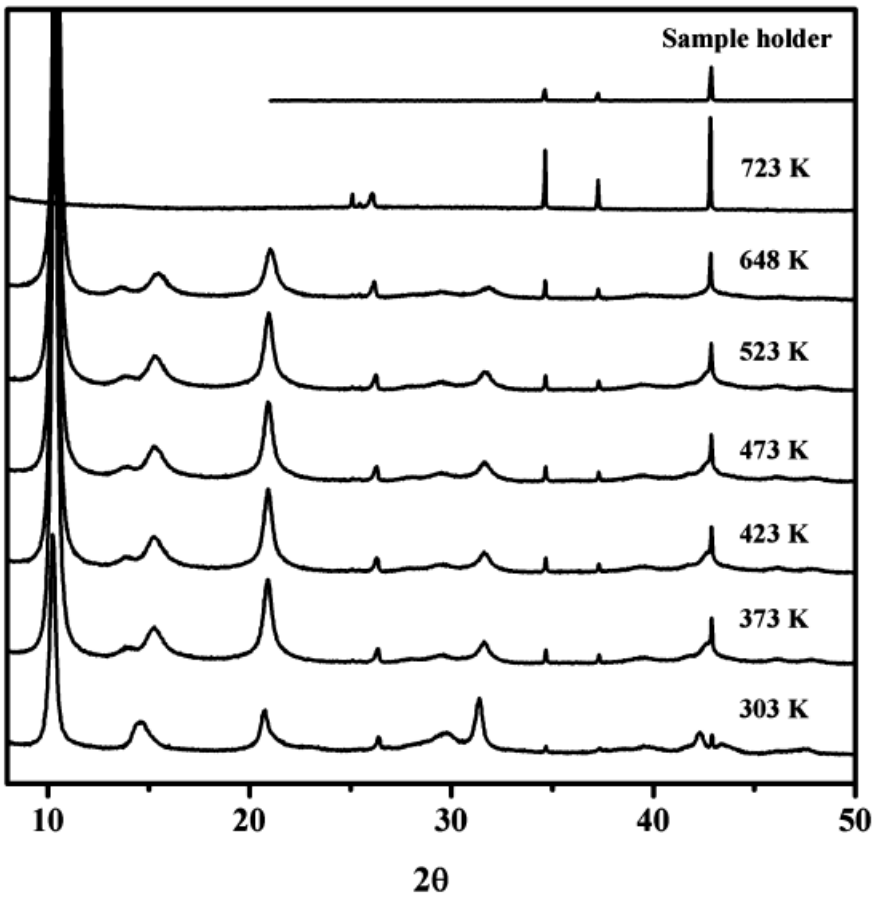

Fig. S20 PXRD of aluminium fumarate MOF at 303, 373, 423, 473, 523, 648 and 723 K and the sample holder (alumina). Reprinted with permission from ref. J. A. Coelho, A. Mafalda Ribeiro, A. F. P. Ferreira, S. M. P. Lucena, A. E. Rodrigues, D. C. S. de Azevedo, *Ind. Eng. Chem. Res*. **2016**, *55*, 2134−2143. Copyright 2016 American Chemical Society.

REFERENCES

1 E. Alvarez, N. Guillou, C. Martineau, B. Bueken, B. Van de Voorde, Cl. Le Guillouzer, P. Fabry, F. Nouar, F. Taulelle, D. de Vos, J.-S. Chang, K. H. Cho, N. Ramsahye, T. Devic, M. Daturi, G. Maurin, C. Serre, *Angew. Chem. Int. Ed*. **2015**, *54*, 3664-3668.

2 A. E. Bennett, C. M. Rienstra, M. Auger, K. V. Lakshmi, R. G. Griffin, Heteronuclear decoupling in rotating solids. *J. Chem. Phys*. **1995**, *103*, 6951-6958.

3 3P INSTRUMENTS, 3P sim, Version 1.1.0.7, Simulation and Evaluation Tool for mixSorb, 3P INSTRUMENTS 2018.

4 A. P. Terzyk, J. Chatłas, P. A. Gauden, G. Rychlicki, P. Kowalczyk, *J. Colloid Interface Sci*. **2003**, *266*, 473-476.